A ribosome-inactivating protein in a Drosophila defensive symbiont

Phineas T. Hamilton, Fangni Peng, Martin J. Boulanger, and Steve J. Perlman

January 2016

The final publication is available at:

https://doi.org/10.1073/pnas.1518648113

Accepted Manuscript:

Hamilton PT, Peng F, Boulanger MJ, Perlman SJ. 2016. A ribosome-inactivating protein in a *Drosophila* defensive symbiont. PNAS. 113:350-355. doi: 10.1073/pnas.1518648113

Classification: Biological Sciences: Ecology and Evolution

Title: A ribosome-inactivating protein in a *Drosophila* defensive symbiont

Short Title: A RIP in a *Drosophila* defensive symbiont

Phineas T. Hamilton[1*], Fangni Peng[2], Martin J. Boulanger[2] and Steve J. Perlman[1,3*]

Author Affiliations:

[1]Department of Biology, University of Victoria, Victoria, BC, Canada, V8W 2Y2.

[2]Department of Biochemistry and Microbiology, University of Victoria, Victoria BC, Canada, V8P 5C2.

[3]Integrated Microbial Biodiversity Program, Canadian Institute for Advanced Research, Toronto ON, Canada, M5G 1Z8.

Corresponding Authors:

Phineas Hamilton; phin.hamilton@gmail.com

Steve Perlman; stevep@uvic.ca

Department of Biology

University of Victoria

PO Box 1700, Station CSC

Victoria BC, Canada, V8W 2Y2

Phone: 250-472-4493

Fax: 250-721-7120

Keywords: symbiosis, male-killing, ribosome-inactivating protein, Shiga toxin, *Hamiltonella, Wolbachia*

Abstract:

Vertically transmitted symbionts that protect their hosts against parasites and pathogens are well known from insects, yet the underlying mechanisms of symbiont-mediated defense are largely unclear. A striking example of an ecologically important defensive symbiosis involves the woodland fly *Drosophila neotestacea*, which is protected by the bacterial endosymbiont *Spiroplasma* when parasitized by the nematode *Howardula aoronymphium*. The benefit of this defense strategy has led to the rapid spread of *Spiroplasma* throughout the range of *D. neotestacea*, though the molecular basis for this protection has been unresolved. Here, we show that *Spiroplasma* encodes a ribosome-inactivating protein (RIP) related to Shiga-like toxins from enterohemorrhagic *E. coli,* and that *Howardula* ribosomal RNA (rRNA) is depurinated during *Spiroplasma*-mediated protection of *D. neotestacea*. First, we show that recombinant *Spiroplasma* RIP catalyzes depurination of 28S ribosomal RNAs in a cell-free assay, as well as *Howardula* rRNA *in vitro* at the canonical RIP target site within the α-sarcin/ricin loop of 28S rRNA. We then show that *Howardula* parasites in *Spiroplasma*-infected flies show a strong signal of rRNA depurination consistent with RIP-dependent modification, and large decreases in the proportion of 28S rRNA intact at the SRL. Notably, host 28S rRNA is largely unaffected, suggesting targeted specificity. Collectively, our study identifies a novel RIP in an insect defensive symbiont, and suggests an underlying RIP-dependent mechanism in *Spiroplasma*-mediated defense.

Significance:

Symbioses between animals and microbes are now recognized as critical to many aspects of host health. This is especially true in insects, which are associated with diverse maternally transmitted endosymbionts that can protect against parasites and pathogens. Here, we find that *Spiroplasma* – a defensive endosymbiont that protects *Drosophila* during parasitism by a virulent and common nematode – encodes a protein toxin, a ribosome-inactivating protein (RIP) related to bacterial virulence factors such as the Shiga-like toxins in *E. coli.* We further find that nematode ribosomal RNA suffers depurination consistent with attack by a RIP when the host is protected by *Spiroplasma*,

suggesting a mechanism through which symbiotic microbes may protect their hosts from disease.

\body

Introduction:

Symbiosis is now recognized to be a key driver of evolutionary novelty and complexity (1, 2), and symbioses between microbes and multicellular hosts are understood as essential to the health and success of diverse lineages, from plants to humans (3). Insects, in particular, have widespread associations with symbiotic bacteria, with most insect species infected by maternally transmitted endosymbionts (4, 5). Though many insect symbionts perform roles essential for host survival, such as supplementing nutrition, others are facultative and not strictly required by their hosts. These facultative symbionts have evolved diverse and intriguing strategies to maintain themselves in host populations despite loss from imperfect maternal transmission and metabolic costs to the host. These range from manipulating host reproduction to increase their own transmission (6, 7), such as by killing male hosts, to providing context-dependent fitness benefits (8). Recently, it has become clear that different insect endosymbionts have independently evolved to protect their hosts against diverse natural enemies that so far include pathogenic fungi (9), RNA viruses (10, 11), parasitoid wasps (12), parasitic nematodes (13), and predaceous spiders (14, 15). This suggests that defense might be a common aspect of many insect symbioses and demonstrates that symbionts can serve as dynamic and heritable sources of protection against natural enemies (8).

Despite a growing appreciation of the importance of symbiont-mediated defense in insects, key questions remain. Most demonstrations of defense have been under laboratory conditions, and the importance of symbiont-mediated protection in natural systems is unclear in most cases (16). At the same time, the proximate causes of defense are largely unknown, although recent studies have provided some intriguing early insights: a *Pseudomonas* symbiont of rove beetles produces a polyketide toxin thought to

deter predation by spiders (14); *Streptomyces* symbionts of beewolves produce antibiotics to protect the host from fungal infection (17); and bacteriophages encoding putative toxins are required for *Hamiltonella defensa* to protect its aphid host from parasitic wasps (18), while the causes of other naturally occurring defensive symbioses are unresolved. From an applied perspective, the ongoing goal of exploiting insect symbioses to arrest disease transmission to humans from insect vectors (19) makes a deeper understanding of the factors contributing to ecologically relevant and evolutionarily durable defensive symbioses urgently needed.

Here, we investigate the mechanism underlying one of the most striking examples of an ecologically important defensive symbiosis. *Drosophila neotestacea* is a woodland fly that is widespread across North America and is commonly parasitized by the nematode *Howardula aoronymphium*. Infection normally sterilizes flies (20); however, when flies harbour a strain of the inherited symbiont *Spiroplasma* – a Gram positive bacterium in the class *Mollicutes* – they remarkably tolerate *Howardula* infection without loss of fecundity, and infection intensity is substantially reduced (13). The benefit conferred by this protection lends a substantial selective advantage to *Spiroplasma*-infected flies, and has led to *Spiroplasma*'s recent spread across North America, with symbiont-infected flies rapidly replacing uninfected ones (21). *Spiroplasma* is a diverse and widespread lineage of arthropod-associated bacteria that can be commensal, pathogenic, or mutualistic (22). Maternal transmission has arisen numerous times in *Spiroplasma*, including strains that are well known as male-killers (22). In addition to defense against nematodes in *D. neotestacea*, other strains of *Spiroplasma* have recently been shown to protect flies and aphids against parasitic wasps and pathogenic fungi, respectively (23–25), but in no case is the mechanism of defense understood.

In theory, there are multiple avenues by which a symbiont may protect its host that include competing with parasites for limiting resources, priming host immunity, or producing factors to directly attack parasites (26). We previously assessed these possibilities in the defensive *Spiroplasma* from *D. neotestacea* (27); our findings best supported a role for toxins in defense, with *Spiroplasma* encoding a highly-expressed putative ribosome-inactivating protein (RIP). RIPs are widespread across plants and some bacteria and include well-known plant toxins of particular human concern such as ricin,

as well as important virulence factors in human toxigenic strains of *E. coli* and *Shigella* (28, 29). RIPs characteristically exert their cytotoxic effects through depurination of eukaryotic 28S ribosomal RNAs (rRNA) at a highly conserved adenine in the α-sarcin/ricin loop (SRL) of the rRNA by cleaving the N-glycosidic bond between the rRNA backbone and adenine (30, 31). While the proliferation of RIPs across different lineages implies functional significance, their ecological roles are unclear, although they often appear to have antiviral or other defensive roles (29, 32). Here, we find that *Spiroplasma* expresses a functional RIP distinct from previously characterized toxins that appears to specifically affect *Howardula* ribosomes in flies coinfected with *Spiroplasma* and *Howardula*. This work suggests the mechanisms employed in defensive associations to protect the host from disease, as well as intriguing ecological roles for RIPs in a tripartite defensive symbiosis.

Results

Spiroplasma strains encode diverse RIP-like sequences

Earlier RNA sequencing assemblies from *Spiroplasma*-infected *D. neotestacea* recovered sequence of a putative RIP encoded in a 403 amino acid ORF (hereafter *Sp*RIP) (27). Characterized RIPs typically belong to one of two classes: type I toxins are monomeric toxins that contain a single catalytically active A chain (typically ~30 kDa). In type II toxins, this A chain is conserved but is additionally linked to a B or B_5 subunit (e.g., for ricin and Shiga-like toxins, respectively) that serves as a lectin and facilitates toxin entry into target cells, typically greatly increasing cytotoxicity (28, 29, 33). The ORF of *Sp*RIP was predicted to encode an N-terminal signal peptide, followed by a disordered region of 70 AAs, and a ~300 AA C-terminal region homologous to characterized RIP A chains. While this is substantially longer than typical for monomeric type I toxins, we found no convincing bioinformatic evidence for the presence of a B chain homologous to those characterized from Shiga-like toxins or type II plant RIPs.

BLASTp searches recovered putative RIPs encoded by other *Spiroplasma* strains, including the recently sequenced defensive and male-killing MSRO strain of *Spiroplasma poulsonii* from *D. melanogaster* (34). Phylogenetic analysis of these protein sequences

with selected seed sequences from the PFAM database (PF00161) placed RIP-like sequences from *Spiroplasma* strains with bacterial RIPs such as the Shiga-like toxins (Figure 1), and alignments confirmed the presence of the known conserved catalytic residues of RIPs in *Sp*RIP (29).

Spiroplasma expresses a functional RIP

To characterize *Sp*RIP, we expressed and purified the protein following codon optimization for *E. coli* (Figure S1; signal peptide removed; Ala31 through His403). This yielded a 44 kDa protein that degraded to a stable protein of 34 kDa after 2 weeks in HBS at 4°C (Figure S1). Consistent with our expectation, mass spectrometric analysis confirmed this to be a result of proteolysis of the ~70 residues of the N-terminal region predicted to be disordered. Subsequent assays were performed using the stable 34 kDa protein that lacked the predicted disordered region.

We used a modified, highly sensitive RT-qPCR based assay to assess depurination activity (35, 36). In brief, depurination at the SRL leaves an abasic site following RIP attack, but does not directly cleave the phosphodiester bond of the sugar phosphate backbone. These assays exploit the property of reverse transcriptases to incorporate dAMP opposite this abasic lesion during reverse transcription, resulting in a quantifiable signature shift from T (the complement of A) to A at the site of depurination in resultant cDNA. To exploit this, we developed qPCR primers to rabbit 28S rRNA for use in cell-free rabbit reticulocyte lysate-based assays.

Incubating reticulocyte lysate with *Sp*RIP led to a ~50% decrease in the abundance of the cDNA representing intact 28S rRNA relative to negative controls (Figure 2A - hereafter intact template; $t_{3.94} = 11.68$, $P < 0.001$), and correspondingly, more than a 1000-fold increase in cDNA representing depurinated rRNA (Figure 2B - hereafter depurinated template; $t_{2.18} = 42.22$, $P < 0.001$). A 4 × 5-fold serial dilution of *Sp*RIP also confirmed depurination across a range of concentrations, with clear dose dependence to < 0.1 μM (Figure 3; linear regression of $\log_2$(depurination) vs. $\log_5$([*Sp*RIP]); $R^2 = 0.88$, $P < 0.001$). This supports the predicted depurination function for *Sp*RIP, with enzyme-dependent depurination likely proceeding through cleavage of the N-glycosidic bond, as is observed in other RIPs.

SpRIP depurinates Howardula ribosomes in vitro

To confirm *Sp*RIP activity against *Howardula* nematode ribosomes, we designed a RT-qPCR assay to measure depurination of *Howardula* rRNA. This assay was able to specifically differentiate *Howardula* rRNA from that of the fly host, with cDNA reverse transcribed from nematode-uninfected fly negative controls yielding no amplification.

We harvested live *Howardula* by gently grinding infected *Drosophila falleni* (*Spiroplasma*-negative) in insect Ringer's solution. We incubated this homogenate, containing viable juvenile nematodes, with recombinant *Sp*RIP at 21°C for 4 hours, using a lower temperature to avoid directly killing nematodes during incubation. Incubation with the toxin again dramatically increased the abundance of depurinated template by more than 2000-fold (Figure 4A & B; $t_{2.38} = 18.34$, $P < 0.001$). In contrast to the reticulocyte lysate assay, there was no substantial decrease in the abundance of intact template under these conditions ($t_{2.94} = 0.51$, $P = 0.65$). We performed a further experiment incubating single nematode motherworms to limit substrate availability, again not observing appreciable depletion of intact 28S rRNA under these conditions, despite large increases in depurinated ribosomes (Figure S2; $t_{3.89} = 0.31$; $t_{2.03} = 8.68$ $P = 0.77$ and $P = 0.01$, respectively), suggesting that a proportion of *Howardula* ribosomes might not be accessible to the stable but truncated recombinant *Sp*RIP used here.

RNA-sequencing shows depurination of Howardula *28S rRNA at the sarcin/ricin loop in the presence of* Spiroplasma

To test for evidence of *Howardula* attack by a RIP *in vivo* we revisited RNA-seq reads generated during a previous experiment, in which we sequenced RNA of *D. neotestacea* and *Howardula* in the presence and absence of *Spiroplasma* infection (27). We reasoned that signal of depurination should be observed in reads mapping to the SRL of *Howardula* 28S rRNA given the reliance of the RNA-seq on reverse transcription during library construction, causing a shift in the sequencing read at the site of depurination.

Mapping raw reads to near full-length 28S rRNA for *Howardula* revealed a highly significant signal of depurination with a shift from A to T (or the complement) in 3.8% of reads mapping to the adenine target of RIPs in *Spiroplasma*-infected flies ($P < 10^{-180}$; coverage = 2,807 reads). In contrast, this signal was not present in *Howardula* reads from *Spiroplasma*-uninfected flies ($P > 0.1$; coverage = 15,389). The same analysis mapping a subset of raw reads to *D. neotestacea* 28S rRNA also revealed significant evidence of depurination, but to a much lesser extent, with a shift detectable in only 0.4% of reads ($P < 10^{-17}$; coverage = 4,822). Again, there was no evidence of depurination in the absence of *Spiroplasma* ($P > 0.1$; coverage = 3,485). This near 10-fold greater depurination of *Howardula* vs. *D. neotestacea* rRNA suggests substantial differences in exposure and/or susceptibility of host vs. parasite ribosomes to a RIP in the presence of *Spiroplasma*, as we would expect. This signal of depurination is also likely conservative; rRNA depurinated by RIPs is highly susceptible to hydrolysis of the sugar-phosphate backbone at the site of depurination (31), and the freezing undergone by these samples prior to library construction might be expected to decrease the detectability of depurination (35). The magnitude of these effects should, however, be interpreted with caution as the polyA RNA enrichment employed prior to sequencing would have depleted rRNA, also potentially affecting the observed signal.

qPCR confirms that Howardula 28S *rRNA is depurinated in vivo during* Spiroplasma *infection.*

We applied the RT-qPCR assay for depurination of *Howardula* 28S rRNA to *Howardula*-infected adult flies, infected and uninfected with *Spiroplasma*, collected 1-day post-eclosion. *Howardula* 28S rRNA with an intact SRL was dramatically decreased in the presence of *Spiroplasma* ($t_{8.88} = 3.37$ $P = 0.008$; Figure 4A). Because this assay is normalized to an upstream region of rRNA not predicted to be affected by RIPs, this represents a ~6-fold depletion of *Howardula* rRNA intact at the SRL in the presence of *Spiroplasma*, relative to the abundance of an upstream region of 28S rRNA. Notably, the depurinated template was also ~20-fold more detectable (Figure 5B; $t_{10.53} = 3.36$ $P = 0.007$) in the presence of *Spiroplasma*. As fold-changes are reported with respect to

control samples with no expected depurination, a decrease of 6-fold in intact SRL would be expected to be a much greater decrease than a 20-fold increase in depurinated template over a (negligible) background signal, although we do not directly measure absolute rRNA abundances. Depurination at the SRL is known to be a potent inducer of apoptosis (33, 37), and as mentioned renders the rRNA backbone highly susceptible to hydrolysis (31), likely accounting for the apparently modest accumulation of depurinated rRNA coincident with a large decrease of relative signal for the intact SRL.

To corroborate RNA-sequencing results and confirm that depurination is more specific to *Howardula,* we designed an RT-qPCR assay for *D. neotestacea* rRNA (Table S1). We assayed fly ovaries – host tissue known to be high in *Spiroplasma* density – in gravid females with and without *Spiroplasma*, as well as in the whole-fly samples that showed depurination of the *Howardula* SRL (above). Though there appeared to be slightly elevated RIP-specific depurination in host rRNA in the presence of *Spiroplasma* (Figures 5C and S3), this was not significant above controls in either assay at these sample sizes ($P = 0.30$ and $P = 0.14$ for whole flies and ovaries, respectively), and was substantially lower than that observed in *Howardula* in the same samples. We also assayed for a signal of depletion of intact template in flies in the presence of *Spiroplasma* similar to that observed for *Howardula*, but observed no such signal (Figure S4, $P = 0.21$), consistent with substantially greater effects on *Howardula.* This confirms the greater level of depurination in the parasite vs. host, suggesting that a RIP disproportionately targets *Howardula* rRNA when *Spiroplasma* is present.

Discussion:

Recent years have seen an increasing awareness that symbiotic associations can be critical in protecting multicellular hosts against parasites and pathogens. Many host-associated microbes produce metabolites that are known or suspected to function in defensive capacities (14, 17, 38), but the effectors that defend against specific enemies in maternally transmitted insect endosymbionts, whose success is typically intimately linked to that of the host (39), are poorly understood. This is largely due to the difficulty of working with uncultivable symbiotic lineages: here neither *Howardula* nor *Spiroplasma* can currently be grown outside of the host, precluding many approaches to establishing

function in these systems. There is great interest in exploiting insect symbioses to interrupt disease transmission from insects to humans, and a lack of understanding of the mechanisms underlying evolutionarily durable defensive symbioses impedes a full evaluation of the efficacy of these strategies.

Here, we show that the *Spiroplasma* defensive symbiont currently sweeping through North American populations of a common woodland *Drosophila* encodes a divergent RIP, and that a virulent and common nematode parasite shows rRNA depurination consistent with RIP attack when *Spiroplasma* is present. While some other facultative symbionts of insects are known to produce potent toxins – such as the pederin produced by *Pseudomonas* symbionts of *Paederus* rove beetles – *Spiroplasma* in *D. neotestacea* is remarkable for the extent to which the association has been selected upon due to its defensive properties, resulting in its rapid spread across North America. It is also remarkable due to the extent to which a prevalent parasite, *Howardula*, is affected. This association thus allows exploration not only of *Spiroplasma*'s defensive factors, but also of ways in which *Howardula* might counter-evolve to mitigate them. Understanding the mechanisms responsible for this defense can thereby clarify the proximate causes of ecologically relevant defensive symbioses, as well as the ways in which they might be circumvented by their targets.

In vivo, depurination of *Howardula* ribosomes occurs to a much greater extent than in the *Drosophila* during *Spiroplasma* infection, demonstrating substantially greater effects on the parasite. Indeed, effective targeting of invading parasites would be expected of a toxin functioning in defense. It is unclear how this specificity is achieved here – there is substantial precedent for specificity of type I plant RIPs, which can have highly varying toxicities against different cell lines *in vitro*, though the molecular basis is mostly unknown (29, but see 30). Similarly, the B_5 subunit of Shiga-like toxins – the closest characterized relatives of *Sp*RIP – binds specifically to the glycosphingolipid Gb3 of mammalian cells, triggering toxin endocytosis into Gb3-bearing cells and leading to heightened toxicity against specific tissues and cell types (30). In the case of *Sp*RIP, whether the predicted disordered region might function similarly as a ligand, specifically binding to receptors of *Howardula* and other parasites is unclear, but is suggested by the lack of a strong decrease in intact rRNA in *in vitro* assays against *Howardula* with

recombinant *Sp*RIP lacking this region. In addition, a potential pore-forming toxin is encoded directly upstream of *Sp*RIP (27), and it might be that such factors provide entry for RIPs into *Howardula* cells, potentiating toxicity.

Intriguingly, *Sp*RIP is the first characterized of what appears to be a relatively diverse array of RIPs encoded by different *Spiroplasma* strains (Figure 1), some of which are primarily known as either insect pathogens or male-killers, and one of which – the MSRO strain of *S. poulsonii* – is also defensive against parasitoid wasps (24). Many, but not all of these putative toxins have retained the essential residues of RIPs, while some also possess extensive modifications that include uncharacterized C-terminal domains of hundreds of amino acids. This conservation and proliferation of RIP-like sequences across *Spiroplasma* strains suggests functional importance in some capacity, and it is tempting to speculate that they might play roles in other defensive symbioses or in male-killing. Indeed, the apoptotic hallmarks of MSRO-induced male-killing bear similarity to those induced by RIPs in other systems (42). Putative Shiga-like toxins are also encoded in the genomes of phages that are essential to the protection against parasitoid wasps that is conferred to aphids by *Hamiltonella* (43), and it will be interesting to test whether these also target ribosomes.

Recent studies that transfer *Spiroplasma* strains to new host species have revealed interesting variation in the fitness consequences and defensive properties of novel host-*Spiroplasma* associations. When established in new host species, the *D. neotestacea* strain of *Spiroplasma* successfully protects against nematode infection (44). On the other hand, although other strains, including at least one predicted to encode RIPs, were able to stably persist in *D. neotestacea*, only the native strain protected against *Howardula* (45), suggesting that particular *Spiroplasma*-encoded RIPs might be specific to different parasites or pathogens. This is consistent with the high degree of divergence observed between *Spiroplasma* RIPs (Figure 1), as well as our finding of *Howardula*-specific depurination. With respect to effects on the host, others have suggested that some degree of mis-targeting of toxins contributes to the virulence that is sometimes observed in novel (laboratory-initiated) *Spiroplasma* infections (46), and our findings are also consistent with this possibility. In *D. neotestacea,* we have observed no fitness costs associated with *Spiroplasma* (e.g. (21)), and population cage experiments also suggest that direct costs of

Spiroplasma – toxin induced or otherwise – are negligible or context dependent in this symbiosis (47).

In sum, we present evidence of a novel RIP encoded by a *Drosophila* defensive symbiont and find that *Howardula* suffers a much greater degree of rRNA depurination than the *Drosophila* host due to *Spiroplasma*; whether RIPs might act in concert with other factors in this association remains to be determined. The continued goal of understanding the complex interactions that underpin ecologically important symbioses require a deeper understanding of these factors, as does the aim of exploiting defensive symbioses to limit disease transmission to humans. Our findings shed light on these factors, while also suggesting an intriguing function for RIPs in nature as players in this tripartite defensive symbiosis.

Materials and methods:

Phylogenetic Analysis

Putative RIPs from *Spiroplasma* were accessed using BLASTp searches against the NCBI nr database with *Sp*RIP as a query, and were included based on a low E-value and high degree of coverage (48). We aligned these and selected RIP sequences from the PFAM seed database using kalign (49) and constructed maximum likelihood trees (1000 bootstraps) with FastTree (50) following model selection in MEGA ((51); WAG).

Expression and Purification of SpRIP

The gene encoding full length *Sp*RIP was codon optimized for expression in *E. coli* and synthesized by GenScript, with the region coding for the mature protein (Ala31 through His403 - signal sequence removed) subcloned into a modified pET28a expression vector containing an N-terminal TEV protease-cleavable hexahistidine tag.

Recombinant *Sp*RIP was produced using the *E. coli* BL21 codon plus strain. Chemically competent cells were transformed and grown in 2XYT media containing 50 μg/ml ampicillin and 35 μg/ml chloramphenicol at 37 °C with shaking. Overnight culture was diluted 20 fold into 1 L ZYP-5052 autoinduction media at the same antibiotic

concentration and grown for 4 hours at 37 °C before the temperature was reduced to 30 °C for overnight cell growth.

Bacterial cells were harvested by centrifugation and lysed by French press. We purified protein in the cell lysate by Ni-NTA batch bind. Briefly, the cell lysate was diluted in a Ni-NTA binding buffer (20 mM HEPES, pH 8.0, 1 M NaCl, 30 mM imidazole), and incubated with 2 ml Ni-NTA slurry at 4 °C for 1 hour with stirring. Following the incubation, the recombinant protein was eluted from Ni-NTA resin in 5 ml fractions with 250 mM imidazole in elution buffer (20 mM HEPES, pH 8.0, 1 M NaCl). Elutions were pooled and buffer exchanged into HEPES-buffered saline (HBS: 20 mM HEPES, pH 7.5, 150 mM NaCl), with 2% glycerol and 0.5 mM EDTA. The N-terminal hexahistidine tag was cleaved with TEV protease using the established protocol from Sigma-Aldrich. The TEV treated RIP was further purified by cation exchange chromatography using 0 - 1.0 M gradient of NaCl in 20 mM HEPES buffer, pH 6.8 and finally by size exclusion chromatography in HBS (20 mM HEPES, pH 7.5, 300 mM NaCl, with 2% glycerol). Fractions were analyzed by SDS-PAGE and the monomeric fractions as defined by SEC elution profile were pooled and concentrated.

Incubation of the purified recombinant protein (44 kDa) at 4 °C for two weeks in HBS resulted in a stable degradation product of 34 kDa as shown by SDS-PAGE (Figure S1). To identify the sequence of the proteolyzed fragment, the 34 kDa band was excised from the gel, reduced, alkylated, and *in silico* digested with trypsin. Mass spectrometric analysis of the digested peptides was done with a Voyager DE-STR mass spectrometer (Applied Biosystems) using mass range 800 – 3500. For comparison with the MS captured peptide masses, the full-length recombinant protein sequence was submitted to Protein Prospector - MS digest server (UCSF), which reports the predicted trypsin-digested peptide masses. The MS data showed that ~70 residues from the N-terminus were proteolyzed.

The final yield of *Sp*RIP was 0.72 mg purified protein L^{-1} cell culture. *BBE31*, a surface protein of *Borrelia burgdorferi*, was purified by the same method and was used alternatively to BSA as a negative control in incubations, showing that *Sp*RIP's activity did not a result from contamination from the expression system.

Bioinformatics for RNA-sequencing

RNA-sequencing reads originating from (27) were used to test for evidence of depurination of the 28S rRNA SRL at the level of cDNA. In brief, a factorial experiment was conducted in which we sequenced the metatranscriptome of *D. neotestacea* in the presence and absence of *Spiroplasma* and *Howardula* infection. Targeted re-assemblies of *Howardula* and *Drosophila* 28s rRNA were conducted in Geneious 7 (Biomatters, Ltd) to obtain near full-length 28S rRNAs spanning the conserved SRL for both species. Raw reads (or a random subset thereof) from *Howardula*-infected libraries with and without *Spiroplasma* were mapped to these assemblies (default low sensitivity setting), and P-values for variants called in Geneious. Raw sequence reads have been deposited under the NBCI SRA PRJNA295093.

Design and validation of RT-qPCR for depurination

For rabbit, *Howardula,* and *Drosophila* ribosomes we designed RT-qPCR assays following the methods of (35, 36) (Table S1). In summary, primers were designed with the 3' terminal base of either the forward or reverse primer complementary to the site of depurination, with separate primers designed to detect intact (A) vs. depurinated (T) template, and a secondary mismatch to increase specificity (35, 36). The reverse primer for each assay was designed in Primer3 (52), and chosen to bind to a region of divergence between *Howardula* and *Drosophila* for those assays. A second normalizing primer set for each assay was designed for upstream rRNA regions not predicted to be affected by RIPs. Because these sequences are contiguous on the rRNA, the normalizing and SRL regions are expected to occur 1:1 in controls (e.g., in the absence of a RIP).

All assays were tested for target specificity using synthetic DNA (IDT gBlocks) with and without a transversion to T at the predicted site of depurination. In all cases, no cross-amplification of the non-target template occurred until ~12 C_t later than target amplification, indicating primer pairs are ~4000× more specific to their target templates, making this the saturation limit of the assay. Because samples with no depurination will cross amplify at this point, fold-changes should be interpreted in a relative manner – changes to reaction conditions that affect specificity will affect baseline measures of depurination. Fold change in targets was calculated using the $\Delta\Delta C_t$ method, normalized

to amplification of rRNA upstream of the site of depurination, and mean C_t values for each target in each separate experiment, or a reference sample from the control treatment when standardizing control samples to 0 was desired (36). If any samples were rerun (for the *in vivo* experiments) ΔC_ts were calculated with respect to a standard of pooled cDNA for normalization across plates. Efficiencies and R^2 values (Table S1) for primers for detection of intact and depurinated template were calculated using 5 × 10-fold serial dilutions of synthetic DNA or random-primed cDNA (for the *Howardula* normalizing primer set only).

Total RNA was extracted from samples (reticulocyte lysate, whole flies, or nematode motherworms) using Trizol (Invitrogen). For each experiment either 500 or 1000 ng of RNA was reverse transcribed using SuperScript II (Invitrogen) and random priming, following quantification with a NanoDrop spectrophotometer. We found that delays in reverse transcription or freeze-thaw cycles decreased detectability of depurinated rRNA, so RNA was reverse transcribed immediately following RNA extraction. qPCR reactions were run at 1/10 cDNA dilutions in duplicate 10 or 20 μL reactions on a BioRad CFX96 thermal cycler with BioRad SsoFast EvaGreen Supermix. Two cDNA samples for tests of *in vivo* depurination which could not be reliably amplified with normalizing primer sets were excluded from analysis (2/21). Control samples with no expected depurination in which the primer set for depurinated template failed to amplify were conservatively assigned the highest reliably amplified C_t value for the primer set for the experiment during analysis. All statistical analyses were conducted in R v.3.2.1 (53), primarily using linear models (Welch's t-test) with $\log_2$ transformations of response variables to meet test assumptions.

For *in vivo* tests of depurination, *Spiroplasma*-infected and uninfected *D. neotestacea* were reared and infected with *Howardula* as detailed in (27).

Acknowledgements:

We thank Perry Howard for constructive discussions, and David Stuss and Matt Ballinger for comments that improved the manuscript. PH was supported by NSERC and UVic Scholarships. This work was supported by NSERC Discovery Grants to SP and MJB and a Sinergia Grant from the Swiss National Science Foundation to SP. MJB

gratefully acknowledges the Canada Research Chair program for salary support. SP is a fellow of the Canadian Institute for Advanced Research's Integrated Microbial Biodiversity Program.

References:

1. Moran NA (2007) Symbiosis as an adaptive process and source of phenotypic complexity. *Proc Natl Acad Sci U S A* 104 Suppl:8627–8633.

2. Moran NA (2006) Symbiosis. *Curr Biol* 16(20):R866–71.

3. McFall-Ngai M, et al. (2013) Animals in a bacterial world, a new imperative for the life sciences. *Proc Natl Acad Sci* 110(9):3229–3236.

4. Zug R, Hammerstein P (2012) Still a host of hosts for *Wolbachia*: analysis of recent data suggests that 40% of terrestrial arthropod species are infected. *PLoS One* 7(6):e38544.

5. Russell JA, et al. (2012) A Veritable Menagerie of Heritable Bacteria from Ants, Butterflies, and Beyond: Broad Molecular Surveys and a Systematic Review. *PLoS One* 7(12):e51027.

6. Werren J, Baldo L, Clark M (2008) *Wolbachia*: master manipulators of invertebrate biology. *Nat Rev Microbiol* 6:741–751.

7. Hunter MS, Perlman SJ, Kelly SE (2003) A bacterial symbiont in the Bacteroidetes induces cytoplasmic incompatibility in the parasitoid wasp *Encarsia pergandiella*. *Proc Biol Sci* 270(1529):2185–90.

8. Jaenike J (2012) Population genetics of beneficial heritable symbionts. *Trends Ecol Evol* 27(4):226–232.

9. Scarborough C, Ferrari J, Godfray H (2005) Aphid protected from pathogen by endosymbiont. *Science* 310:1781.

10. Teixeira L, Ferreira A, Ashburner M (2008) The bacterial symbiont *Wolbachia* induces resistance to RNA viral infections in *Drosophila melanogaster*. *PLoS Biol* 6(12):e2.

11. Hedges LM, Brownlie JC, O'Neill SL, Johnson KN (2008) *Wolbachia* and virus protection in insects. *Science* 322(5902):702.

12. Oliver KM, Russell JA, Moran NA, Hunter MS (2003) Facultative bacterial symbionts in aphids confer resistance to parasitic wasps. *Proc Natl Acad Sci U S A* 100(4):1803–7.

13. Jaenike J, Unckless R, Cockburn SN, Boelio LM, Perlman SJ (2010) Adaptation via Symbiosis: Recent Spread of a *Drosophila* Defensive Symbiont. *Science (80-)* 329(5988):212–215.

14. Piel J (2002) A polyketide synthase-peptide synthetase gene cluster from an uncultured bacterial symbiont of Paederus beetles. *Proc Natl Acad Sci U S A* 99(22):14002–7.

15. Kellner RLL, Dettner K (1996) Differential efficacy of toxic pederin in deterring potential arthropod predators of *Paederus (*Coleoptera: Staphylinidae) offspring. *Oecologia* 107(3):293–300.

16. Oliver KM, Smith AH, Russell JA (2013) Defensive symbiosis in the real world - advancing ecological studies of heritable, protective bacteria in aphids and beyond. *Funct Ecol* 28(2):341–355.

17. Kroiss J, et al. (2010) Symbiotic streptomycetes provide antibiotic combination prophylaxis for wasp offspring. *Nat Chem Biol* 6(4):261–263.

18. Oliver KM, Degnan PH, Hunter MS, Moran NA (2009) Bacteriophages encode factors required for protection in a symbiotic mutualism. *Science (80-)* 325(5943):992–4.

19. Hoffmann AA, et al. (2011) Successful establishment of *Wolbachia* in *Aedes* populations to suppress dengue transmission. *Nature* 476(7361):454–7.

20. Jaenike J (1995) Interactions between and their mycophagous nematode *Drosophila* to community parasites: from physiological to community ecology. *Oikos* 72(2):235–244.

21. Cockburn SN, et al. (2013) Dynamics of the continent-wide spread of a *Drosophila* defensive symbiont. *Ecol Lett* 16(5):609–16.

22. Anbutsu H, Fukatsu T (2011) *Spiroplasma* as a model insect endosymbiont. *Environ Microbiol Rep* 3(2):144–53.

23. Xie J, Vilchez I, Mateos M (2010) Spiroplasma bacteria enhance survival of *Drosophila hydei* Attacked by the parasitic wasp *Leptopilina heterotoma*. *PLoS One* 5(8):e12149.

24. Xie J, Butler S, Sanchez G, Mateos M (2014) Male killing *Spiroplasma* protects *Drosophila melanogaster* against two parasitoid wasps. *Heredity* 112(4):399–408.

25. Lukasik P, van Asch M, Guo H, Ferrari J, Godfray HCJ (2013) Unrelated facultative endosymbionts protect aphids against a fungal pathogen. *Ecol Lett* 16(2):214–8.

26. Haine ER (2008) Symbiont-mediated protection. *Proc R Soc B Biol Sci* 275(1633):353–361.

27. Hamilton PT, Leong JS, Koop BF, Perlman SJ (2014) Transcriptional responses in a *Drosophila* defensive symbiosis. *Mol Ecol* 23:1558–1570.

28. Bergan J, Dyve Lingelem AB, Simm R, Skotland T, Sandvig K (2012) Shiga toxins. *Toxicon* 60(6):1085–1107.

29. De Virgilio M, Lombardi A, Caliandro R, Fabbrini MS (2010) Ribosome-inactivating proteins: from plant defense to tumor attack. *Toxins (Basel)* 2(11):2699–737.

30. Stirpe F (2004) Ribosome-inactivating proteins. *Toxicon* 44(4):371–383.

31. Endo Y, Tsurugi K (1986) Mechanism of action of ricin and related toxic lectins on eukaryotic ribosomes. *Nucleic Acids Symp Ser* 262(17):187–190.

32. Lainhart W, Stolfa G, Koudelka GB (2009) Shiga toxin as a bacterial defense against a eukaryotic predator, Tetrahymena thermophila. *J Bacteriol* 191(16):5116–5122.

33. Johannes L, Römer W (2010) Shiga toxins — from cell biology to biomedical applications. *Nat Rev Microbiol* 8(2):105–16.

34. Paredes JC, et al. (2015) Genome sequence of the *Drosophila melanogaster* male-killing *Spiroplasma* strain MSRO endosymbiont. *Am Soc Microbiol* 6(2):1–12.

35. Melchior WB, Tolleson WH (2010) A functional quantitative polymerase chain reaction assay for ricin, Shiga toxin, and related ribosome-inactivating proteins. *Anal Biochem* 396(2):204–211.

36. Pierce M, Kahn JN, Chiou J, Tumer NE (2011) Development of a quantitative RT-PCR assay to examine the kinetics of ribosome depurination by ribosome inactivating proteins using *Saccharomyces cerevisiae* as a model. *RNA* 17(1):201–210.

37. Iordanov MS, et al. (1997) Ribotoxic stress response: activation of the stress-activated protein kinase JNK1 by inhibitors of the peptidyl transferase reaction and by sequence-specific RNA damage to the alpha-sarcin/ricin loop in the 28S rRNA. *Mol Cell Biol* 17(6):3373–3381.

38. Nakabachi A, et al. (2013) Defensive bacteriome symbiont with a drastically reduced genome. *Curr Biol*:1–7.

39. Hamilton PT, Perlman SJ (2013) Host defense via symbiosis in *Drosophila*. *PLoS Pathog* 9(12):1–4.

40. Sandvig K, van Deurs B (2005) Delivery into cells: lessons learned from plant and bacterial toxins. *Gene Ther* 12(11):865–872.

41. Chan WY, Huang H, Tam SC (2003) Receptor-mediated endocytosis of trichosanthin in choriocarcinoma cells. *Toxicology* 186(3):191–203.

42. Harumoto T, Anbutsu H, Fukatsu T (2014) Male-Killing *Spiroplasma* Induces Sex-Specific Cell Death via Host Apoptotic Pathway. *PLoS Pathog* 10(2). doi:10.1371/journal.ppat.1003956.

43. Degnan PH, Moran NA (2008) Diverse phage-encoded toxins in a protective insect endosymbiont. *Appl Environ Microbiol* 74(21):6782–6791.

44. Haselkorn TS, Cockburn SN, Hamilton PT, Perlman SJ, Jaenike J (2013) Infectious adaptation: Potential host range of a defensive endosymbiont in *Drosophila*. *Evolution (N Y)* 67(4):934–945.

45. Haselkorn TS, Jaenike J (2015) Macroevolutionary persistence of heritable endosymbionts: acquisition, retention, and expression of adaptive phenotypes in *Spiroplasma*. *Mol Ecol* 24(14):3752–3765.

46. Nakayama S, et al. (2015) Can maternally inherited endosymbionts adapt to a novel host? Direct costs of *Spiroplasma* infection, but not vertical transmission efficiency, evolve rapidly after horizontal transfer into *D. melanogaster*. *Heredity* 114(6):539–543.

47. Jaenike J, Brekke TD (2011) Defensive endosymbionts: a cryptic trophic level in community ecology. *Ecol Lett* 14(2):150–5.

48. Altschul SF, et al. (1997) Gapped BLAST and PSI-BLAST: a new generation of protein database search programs. *Nucleic Acids Res* 25(17):3389–402.

49. Lassmann T, Sonnhammer ELL (2005) Kalign--an accurate and fast multiple sequence alignment algorithm. *BMC Bioinformatics* 6:298.

50. Price MN, Dehal PS, Arkin AP (2009) Fasttree: Computing large minimum evolution trees with profiles instead of a distance matrix. *Mol Biol Evol* 26(7):1641–1650.

51. Tamura K, et al. (2011) MEGA5: Molecular evolutionary genetics analysis using maximum likelihood, evolutionary distance, and maximum parsimony methods. *Mol Biol Evol* 28(10):2731–2739.

52. Koressaar T, Remm M (2007) Enhancements and modifications of primer design program Primer3. *Bioinformatics* 23(10):1289–91.

53. R Core Team (2014) R: A Language and Environment for Statistical Computing. Available at: http://www.r-project.org/.

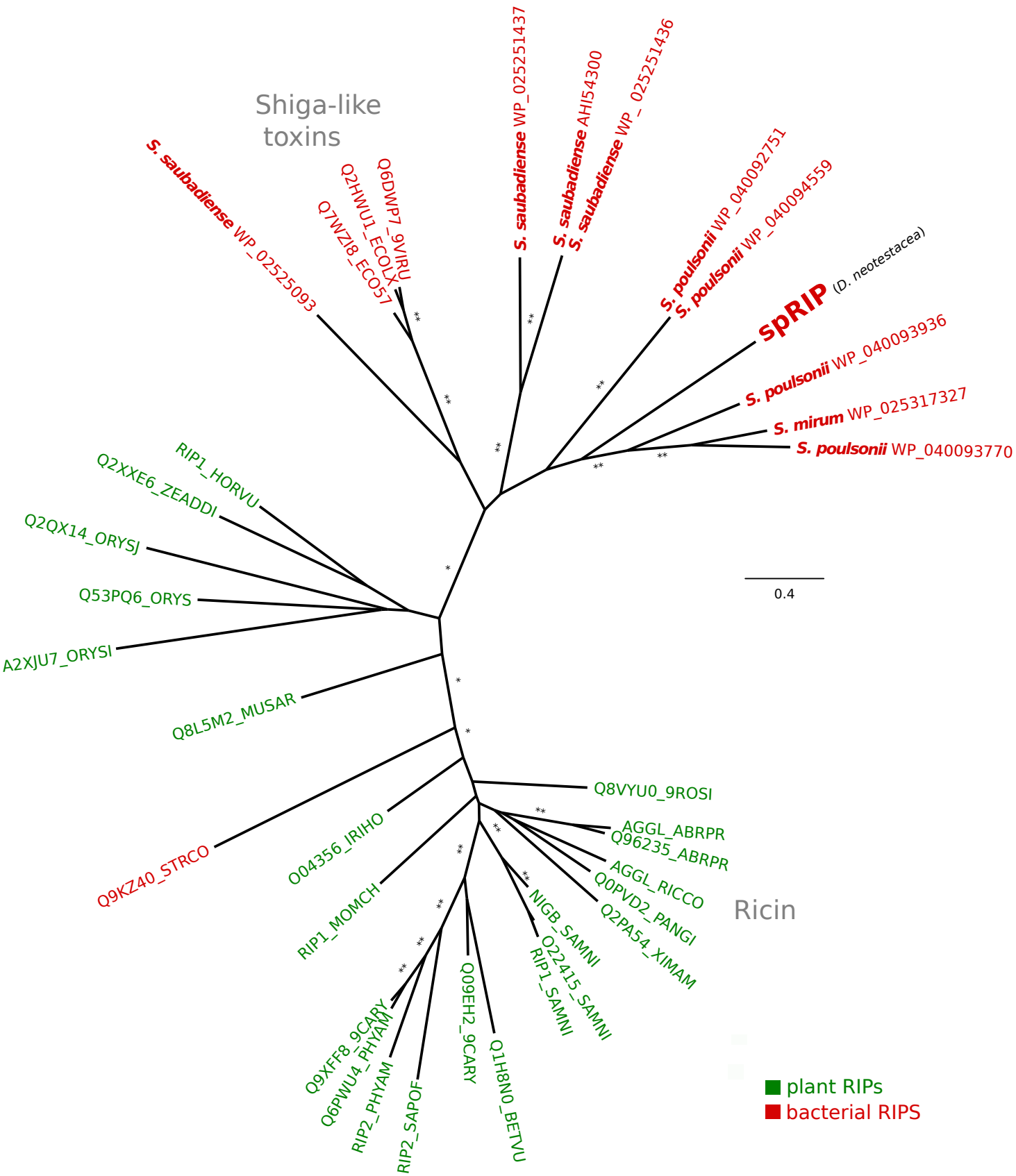
Shiga-like toxins
S. saubadiense WP_02525093
Q7WZI8_ECO57
Q2HWU1_ECOLX
Q6DWP7_9VIRU
S. saubadiense WP_025251437
S. saubadiense AHI54300
S. saubadiense WP_025251436
S. poulsonii WP_040092751
S. poulsonii WP_040094559
spRIP (D. neotestacea)
S. poulsonii WP_040093936
S. mirum WP_025317327
S. poulsonii WP_040093770
RIP1_HORVU
Q2XXE6_ZEADDI
Q2QX14_ORYSJ
Q53PQ6_ORYS
A2XJU7_ORYSI
Q8L5M2_MUSAR
Q9KZ40_STRCO
O04356_IRIHO
RIP1_MOMCH
Q8VYU0_9ROSI
AGGL_ABRPR
Q96235_ABRPR
AGGL_RICCO
Q0PVD2_PANGI
Q2PA54_XIMAM
NIGB_SAMNI
Q22415_SAMNI
RIP1_SAMNI
Q09EH2_9CARY
Q1H8N0_BETVU
Q9XFF8_9CARY
Q6PWU4_PHYAM
RIP2_PHYAM
RIP2_SAPOF
Ricin
0.4
plant RIPs
bacterial RIPS

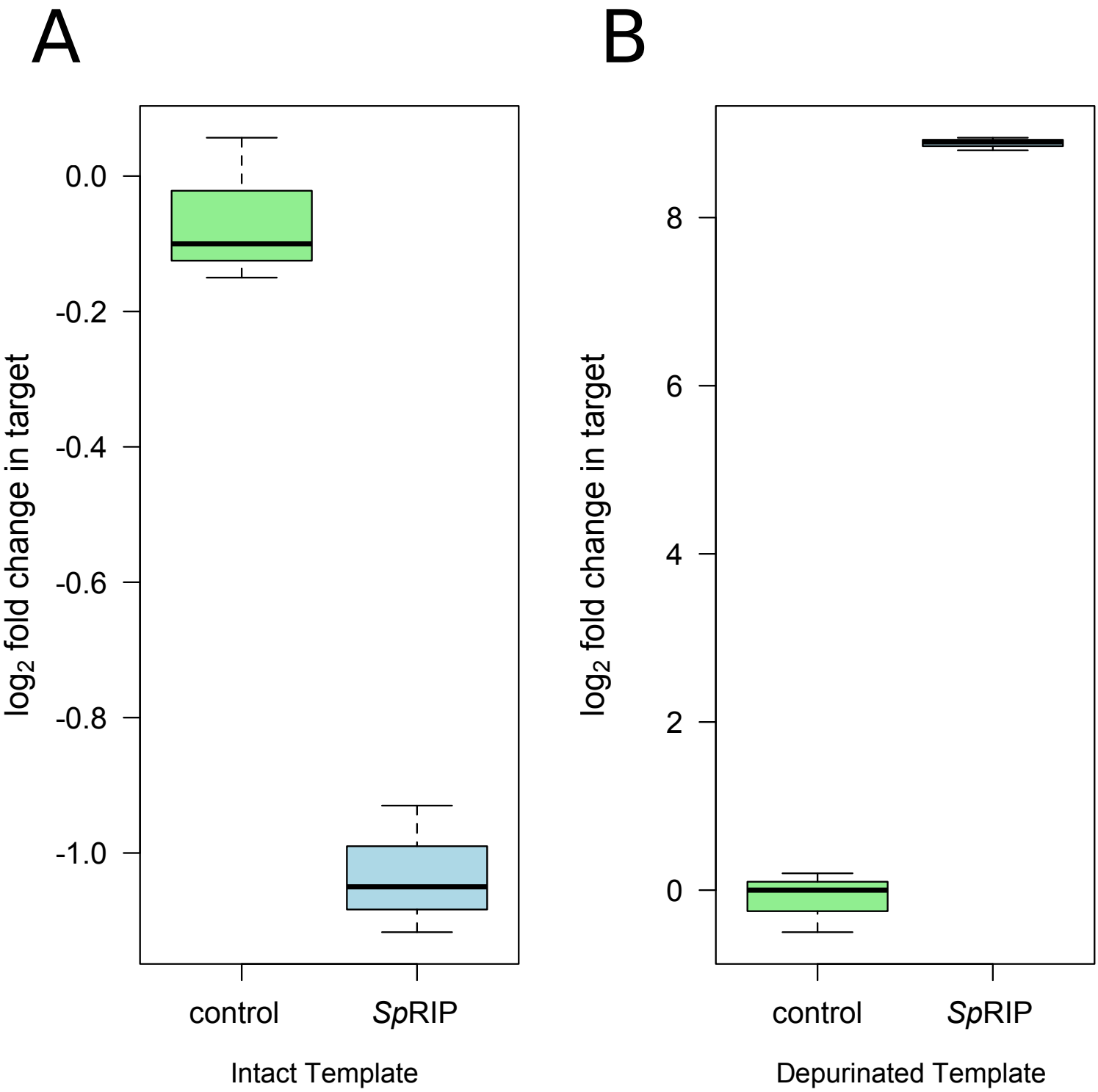
A
B
0.0
-0.2
-0.4
-0.6
-0.8
-1.0
log2 fold change in target
8
6
4
2
0
log2 fold change in target
control
SpRIP
Intact Template
control
SpRIP
Depurinated Template

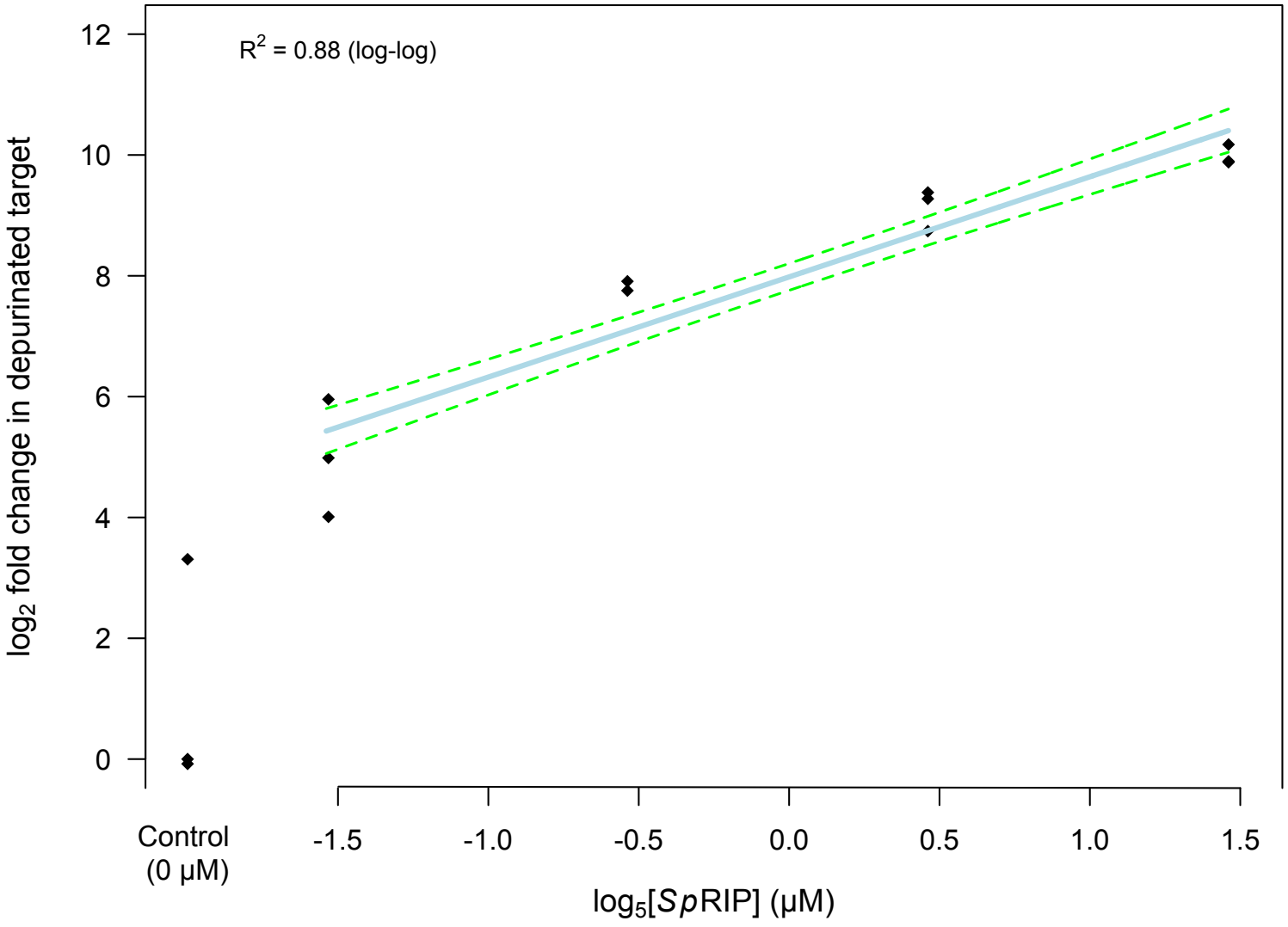
R^2 = 0.88 (log-log)
$\log_2$ fold change in depurinated target
12
10
8
6
4
2
0
Control
(0 μM)
-1.5
-1.0
-0.5
0.0
0.5
1.0
1.5
$\log_5$[*Sp*RIP] (μM)

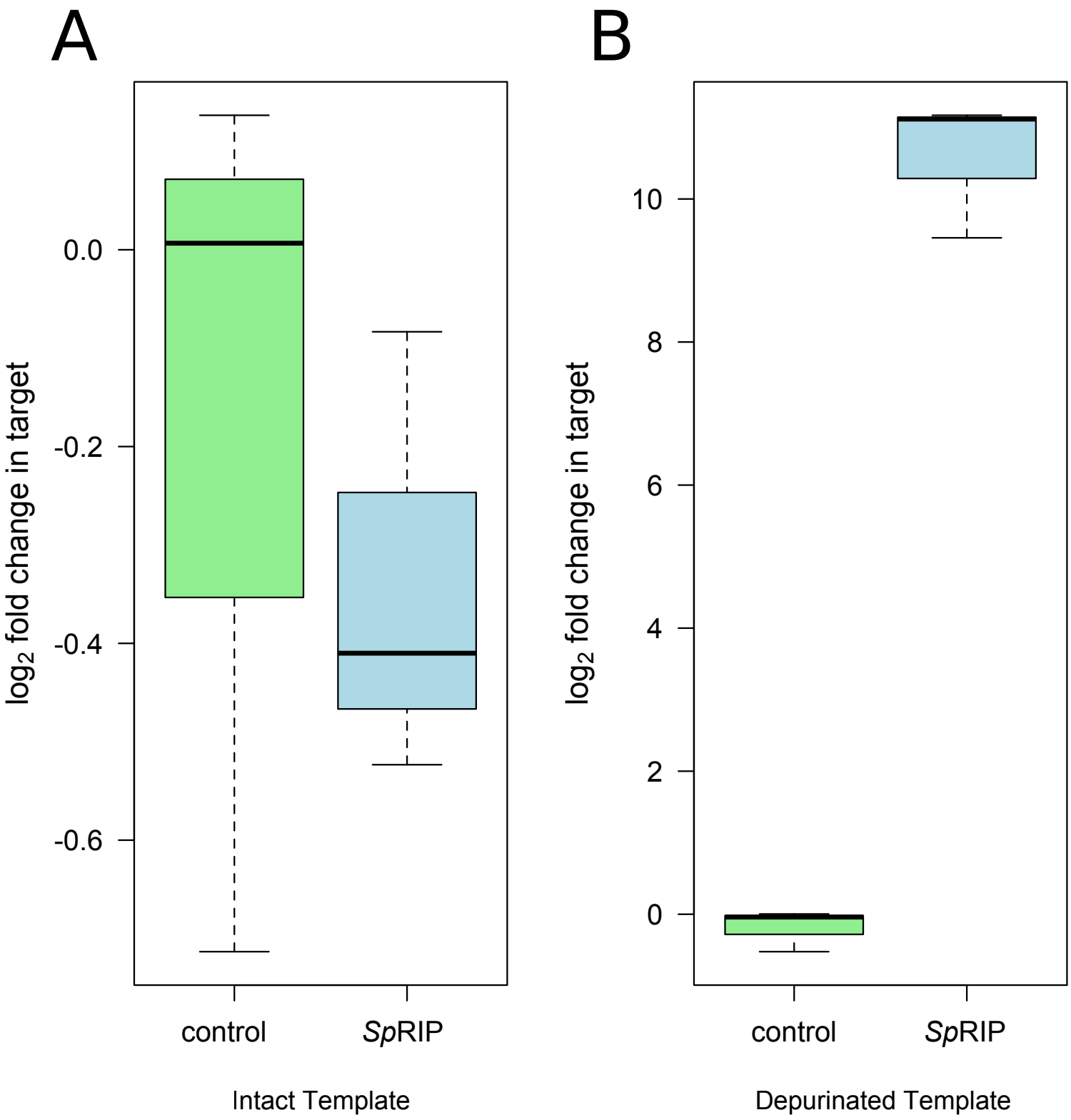
A
B
0.0
-0.2
-0.4
-0.6
log2 fold change in target
10
8
6
4
2
0
log2 fold change in target
control
SpRIP
control
SpRIP
Intact Template
Depurinated Template

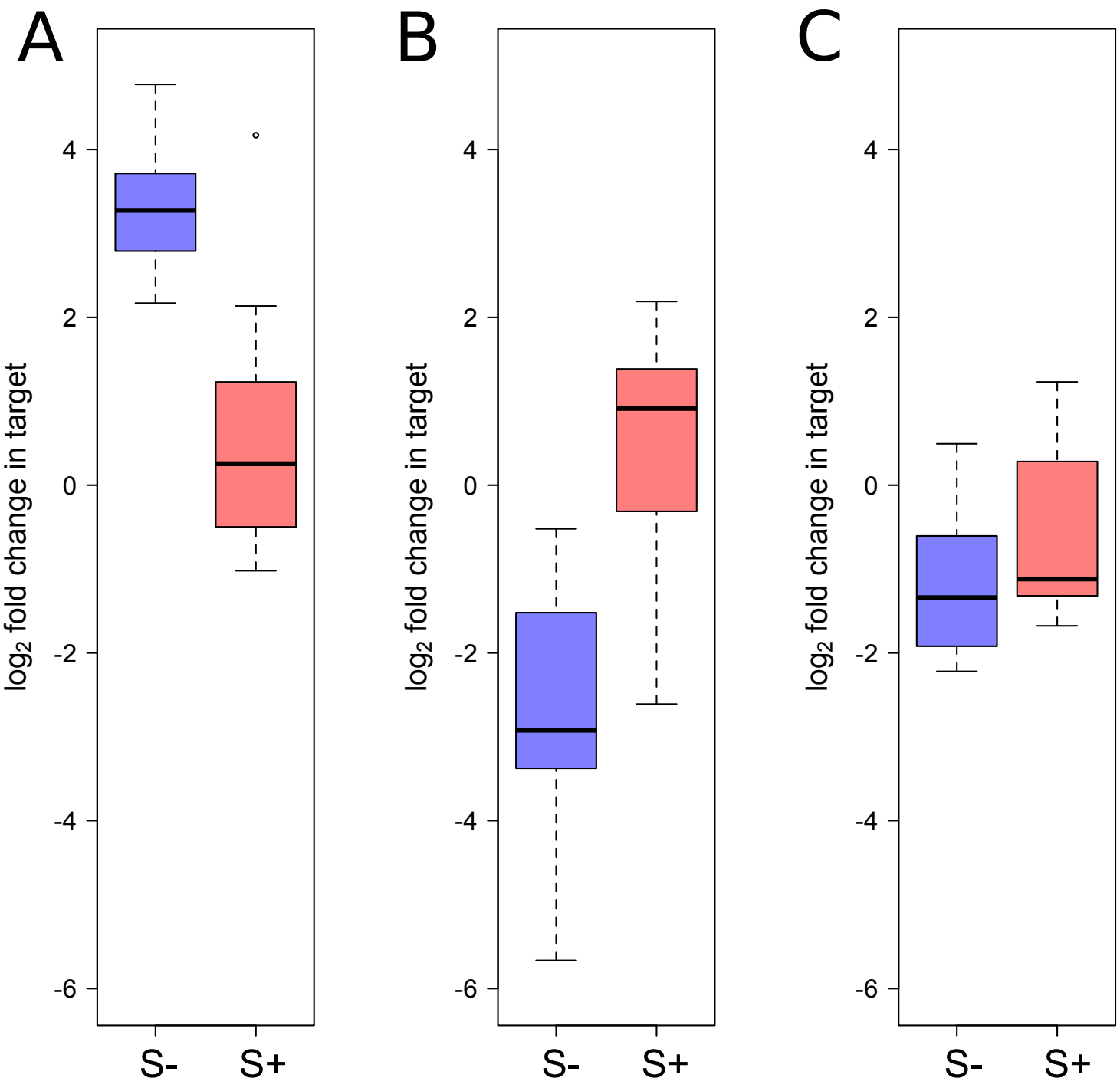
A
B
C
log2 fold change in target
4
2
0
-2
-4
-6
S-
S+

Supplemental Figures and Tables

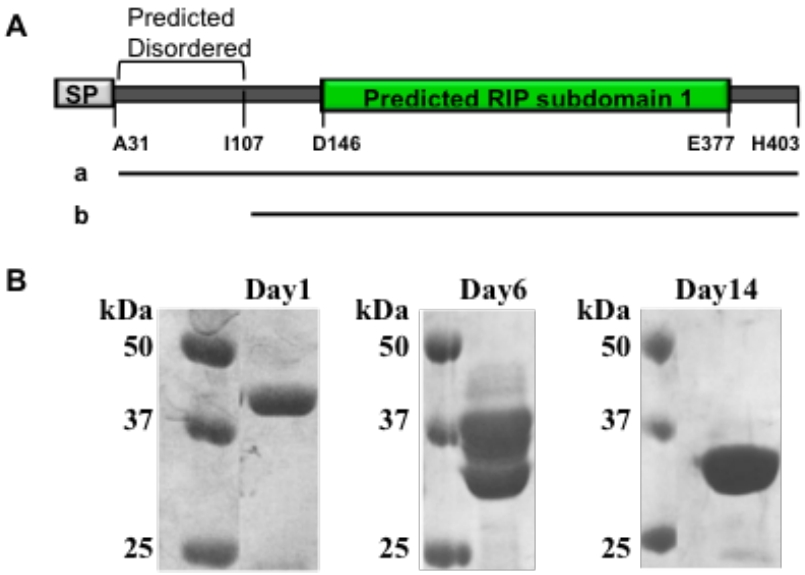

Figure S1. The purified recombinant *Sp*RIP degraded into a stable product over two weeks time at 4°C. **(A)** Schematic of *Sp*RIP domain prediction. SP, signal peptide. Black horizontal line **a** represents the recombinant protein (Ala31 to His403) produced in this study. **b** represents the stable degradation product from purified recombinant *Sp*RIP. **(B)** SDS-PAGE analysis of the purified recombinant *Sp*RIP (44 kDa) incubated at 4 °C over time. The final stable degradation product (~34 kDa on Day 14 gel) was analyzed by mass spectrometry.

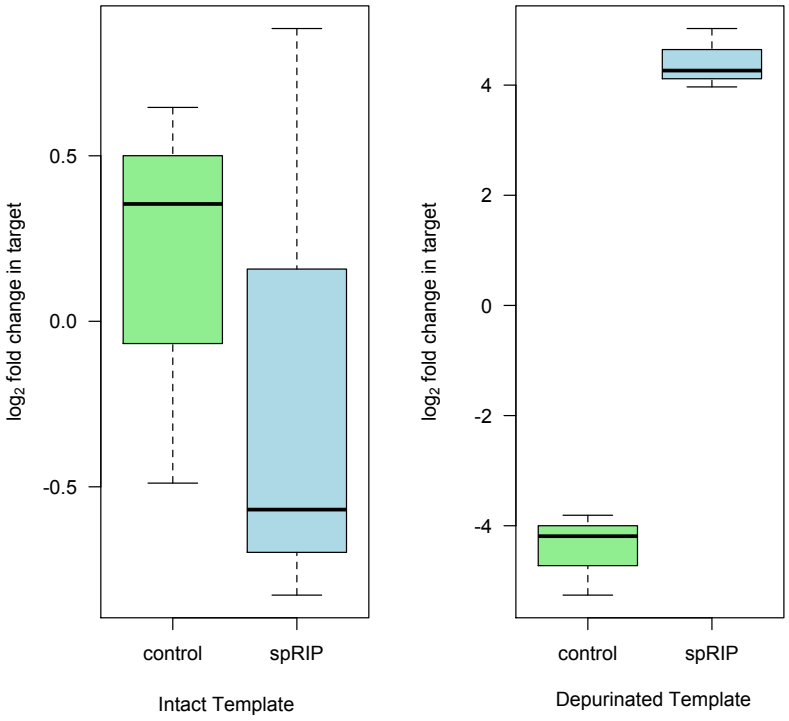

Figure S2. Incubation of single *Howardula* motherworms with *Sp*RIP for 4 hours leads to an increase in cDNA representing depurinated *Howardula* 28S rRNA, but no decrease in intact rRNA (P = 0.01 and 0.77, respectively; N = 6)

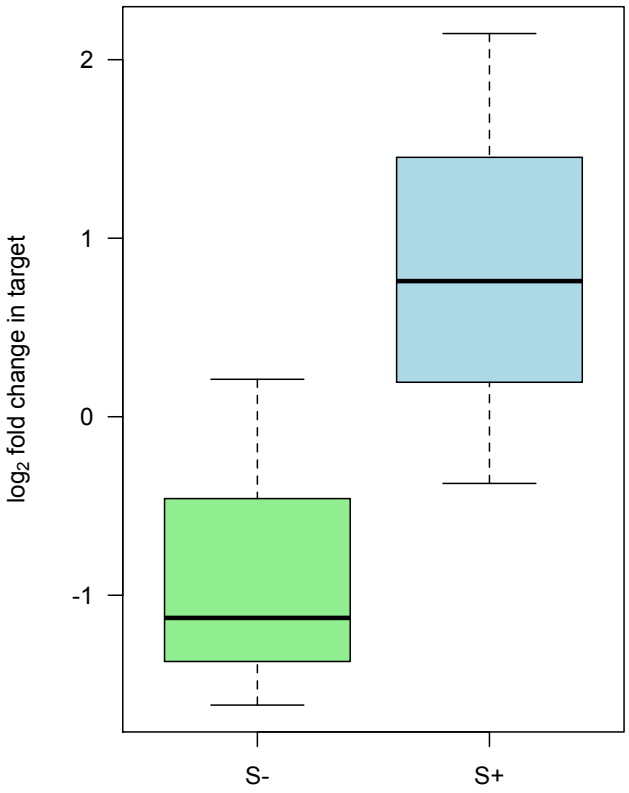

Figure S3. Ribosomal RNA in *D. neotestacea* ovaries is not strongly depurinated at the site of RIP attack in the presence of *Spiroplasma* (S+) (N = 6; P = 0.14). Abundance of depurinated template normalized to upstream rRNA presented. Ovaries were dissected from 1-2 week old gravid females.

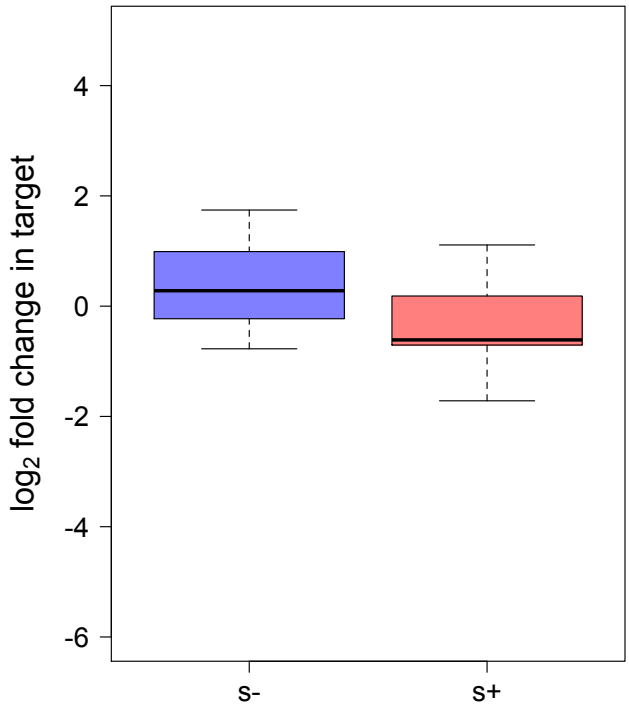

Figure S4. *Drosophila neotestacea* 28S rRNA does not show appreciable depletion of signal of 28S rRNA intact at the sarcin/ricin loop in the presence of *Spiroplasma* (S- vs. S+) (P = 0.21; N= 13), in contrast to the strong signal of depletion observed in *Howardula* rRNA from the same flies (Figure 5).

Table S1. Efficiencies of primers used for all assays. Efficiency and specificity were validated on standard curves of 5 × 10-fold serial dilutions of synthetic DNA (IDT gBlocks) for all primer sets, except for the primer pair for the *Howardula* normalizing primer set, which was tested using a dilution series of cDNA reverse transcribed from *Howardula*-infected flies. Bases specific to sites of depurination are in bold, and deliberate mismatches underlined.

Primer Set	**Primer Sequences (forward and reverse, 5' to 3')**	**R^2**	**Efficiency**	**Slope 95% CI**
	Drosophila			
intact	CGACAGCATTCCTGCGTAGTAAG**A** ACAATGCAAATTGCCCCTTA	0.995	106.6 %	-3.34 < *s* < -3.01
depurinated	CGACAGCATTCCTGCGTAGTAAG**T** ACAATGCAAATTGCCCCTTA	0.997	101.4 %	-3.44 < *s* < -3.13
normalizer	CAAGGACATTGCCAGGTAGG AGCTTTTGCTGTCCCTGTGT	0.997	102.7 %	-3.40 < *s* < -3.12
	Howardula			
intact	TGATAGTAATCCTGCTTAGTAAG**A** CACCGGAGAGCAACGATATT	0.997	98.0 %	-3.52 < *s* < -3.22
depurinated	TGATAGTAATCCTGCTTAGTAAG**T** CACCGGAGAGCAACGATATT	0.998	105.4 %	-3.32 < *s* < -3.08
normalizer	CAAATGCCTCGTCGGATG GCCAAAGCCTCCCACTTATAC	0.991	92.1 %	-3.81 < *s* < -3.24
	Rabbit			
intact	GGGTTTAGACCGTCGTGAGA **A**GTGGAACCGCAGGTTCAGA	0.998	79.6 %	-4.03 < *s* < -3.83
depurinated	GGGTTTAGACCGTCGTGAGA **T**GTGGAACCGCAGGTTCAGA	0.997	78.9 %	-4.13 < *s* < -3.80
normalizer	CGTTGGATTGTTCACCCACT CATACACCAAATGTCTGAACCTG	0.999	96.4 %	-3.48 < *s* < -3.33